ACS OMEGA

http://pubs.acs.org/journal/acsodf

Article

Platinum Complexes from C−H Activation of Sterically Hindered [C^N] Donor Benzothiophene Imine Ligands: Synthesis and Photophysical Properties

Craig M. Anderson,* Belle Coffey, Leslie Morales, Matthew W. Greenberg, Matthew Norman, Michael Weinstein, Garrett Brown, and Joseph M. Tanski

Cite This: *ACS Omega* 2020, 5, 26855−26863

Read Online

ACCESS | Metrics & More | Article Recommendations | Supporting Information

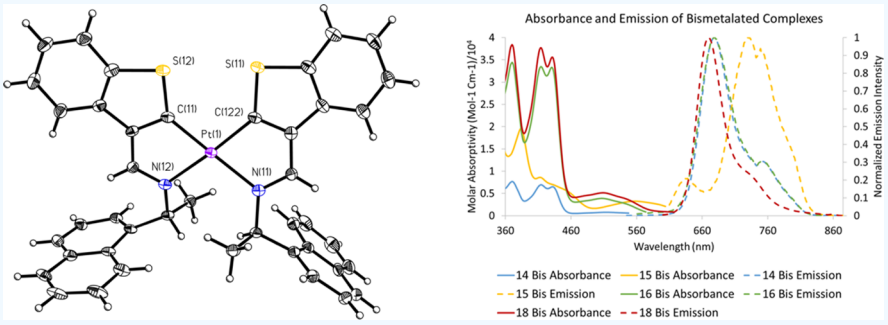

ABSTRACT: Primary amines and benzothiophene-3-carboxaldehyde were reacted to give four large, bulky imine ligands. These imine ligands were reacted with a tetramethyl platinum dimer and by heteroatom-assisted C−H activation, both monometalated compounds and bismetalated compounds were synthesized. In all cases, five-membered platinacycles were formed. The compounds were characterized by NMR spectroscopy, and one bismetalated compound was characterized by single-crystal X-ray diffraction. The UV−vis absorption and emission spectra and the excited-state lifetimes were recorded for these complexes. Density functional theory (DFT) and time-dependent-DFT calculations were performed to aid in the assignment of the absorption and emission spectra of the newly synthesized complexes.

INTRODUCTION

Cyclometalated complexes, including platinum species are known for their interesting catalytic and photophysical properties.[1,2] The properties of these cyclometalated compounds are also studied for their applications in a variety of fields, including sensors and devices.[3,4] Generally cyclometalation is achieved by C−H activation of an ortho proton often by chelate assistance.[5] Strong field ligands with carbon donors, the rigidity of the conjugated ring system, and the strong spin−orbit coupling of the heavy-metal center are explanations for the favorable photophysical properties of cyclometalated compounds, including long-lived excited triplet states.[6−8] Thiophenes are also known for their photophysical properties and are implicated in a variety of applications, including solar cells and photodetectors.[9−11] Benzothiophenes are thiophenes with an additional fused aromatic ring. Benzothiophene fragments are known in pharmaceuticals and dyes and thus have been studied.[12−18] The additional size and conjugation may enhance the desirable properties of the cyclometalated complexes with benzothiophene-derived ligands. Bismetalated complexes are less studied than their monometalated analogues;[19−21] however, perhaps with the additional strong field chelates, C^N ligands may improve the properties of these cyclometaled species.[22] Computational studies on metal compounds have advanced a great deal in the last decade.[23−25] Computational results for large compounds were computationally expensive, taking a great deal of time and results were often suspect, suggesting that synthesis precede computation.[26] Recently, commercially available density functional theory (DFT) packages have become much more inviting and accessible with results allowing for the prediction of properties, such as assignment of electronic spectra bands in platinum compounds.[27−30] We have undertaken the synthesis of several biscyclometalated platinum species, measured their photophysical properties, and used DFT computational results to aid in the assignment of the transitions in the electronic spectra.

Received: August 19, 2020
Accepted: September 28, 2020
Published: October 8, 2020

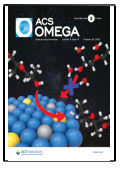

https://dx.doi.org/10.1021/acsomega.0c03993
ACS Omega 2020, 5, 26855−26863

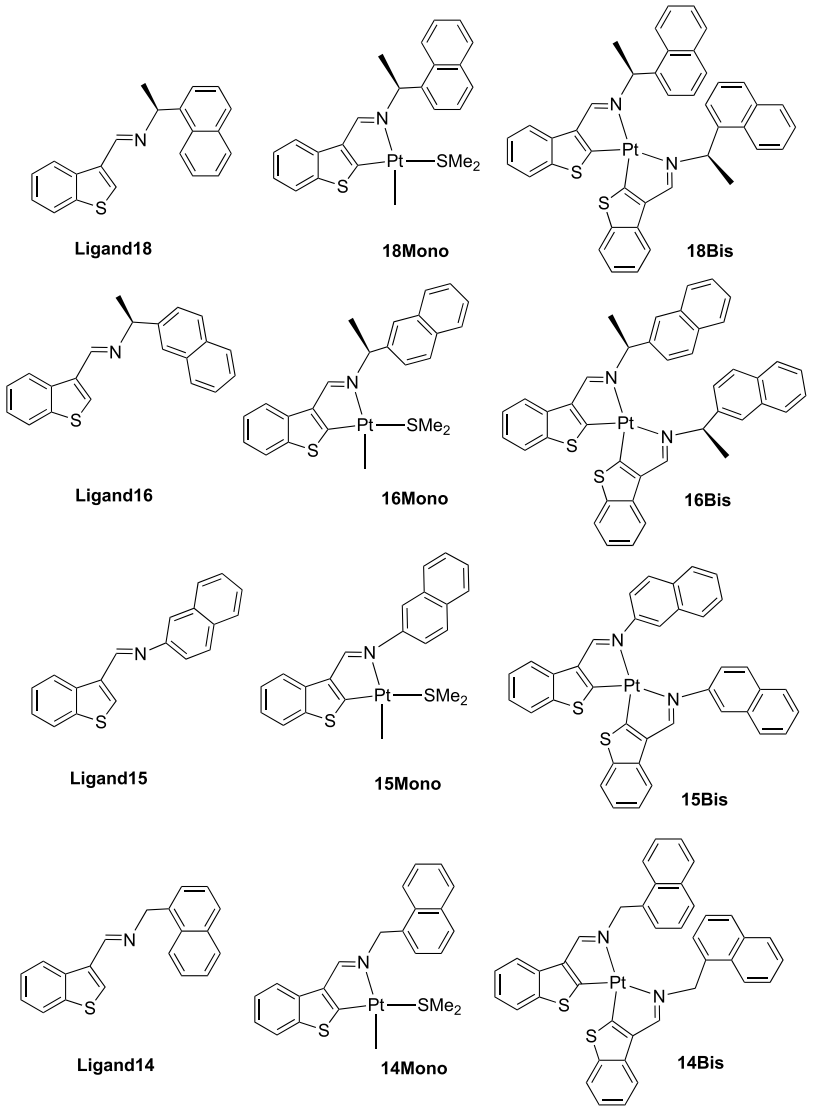

Figure 1. Structures for ligands and monometalated and bismetalated compounds.

RESULTS AND DISCUSSION

The four ligands (Figure 1) utilized in this study were synthesized by condensation reactions of the appropriate amine and aldehyde. The four ligands were characterized by ^{1}H and ^{13}C NMR spectroscopy. The monometalated compounds (Figure 1) were synthesized with one equivalent of ligand per platinum center, utilizing compound $[Pt_2Me_4(\mu\text{-}SMe_2)_2]$, **PtA**, either by stirring the reactants in solution or in a microwave reactor, while bismetalated compounds (Figure 1) were synthesized with two equivalents of ligands per metal center in a solution of refluxing toluene. **18Bis**, seemingly the compound with the bulkiest of ligands, could also be synthesized in methylene chloride at room temperature over a period of several days, whereas none of the other bismetalated species could be obtained under the same conditions. All compounds formed five-membered metalated platinacycles, with the bis compounds forming two such metalacycles. The platinum metalacycle compounds were mainly characterized by 1D and 2D NMR and HRMS. An X-ray diffraction (XRD) study on a single crystal of **18Bis** corroborated its molecular structure (Figure 2) as assigned using the NMR spectral data. Several pieces of data led to the

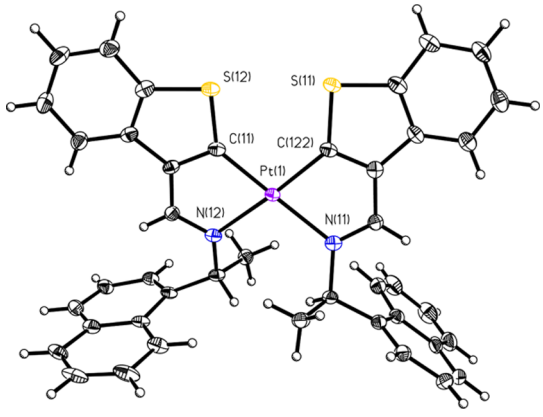

Figure 2. ORTEP of compound **18Bis** (50% probability thermal ellipsoids). Selected bonds lengths (Å) and angles (°): Pt–N(11): 2.136 (4); Pt–N(12): 2.158 (4); Pt–C(122):1.982 (6); Pt–C(11): 1.972 (7); C(11)–Pt–C(122): 99.4 (3); C(11)–Pt–N(12): 79.2(2); C(122)–Pt–N(12): 170.69 (19); C(11)–Pt–N(11): 171.87 (19); C(122)–Pt–N(11):77.9 (2); N(11)–Pt–N(12): 104.68 (14).

https://dx.doi.org/10.1021/acsomega.0c03993
ACS Omega 2020, 5, 26855−26863

NMR resonance assignments of the bis species. For example, no platinum-methyl resonances were observed once two chelate ligands were metalated. A few good diagnostic peaks are available in these compounds, one being the imine resonance at around 8.2 ppm.

Additional diagnostic resonances due to protons on the chelate ligand are useful, including the α-methyl and methine resonances. For example, the proton NMR spectrum of the **18Bis** compound has the imine, methine, and α-methyl resonances observed at 8.23 [^3J(Pt−H) = 71 Hz], 6.06, and 1.80 ppm, respectively, all reasonable for platinum(II) compounds.[31−35] The monometalated species also contain the ancillary methyl and dimethylsulfide ligands in the platinum coordination sphere, along with the chelate C^N ligand, allowing for additional diagnostic resonances in the NMR spectra to aid in characterization of these species. For example, the proton NMR spectrum of the **18Mono** compound has the imine, methine, dimethylsulfide, α-methyl, and the platinum-methyl resonances observed at 8.74, 6.10, 1.91, 1.86, and 1.19 ppm, respectively, with ^3J(Pt−H), ^3J(H−H), ^3J(Pt−H), ^3J(H−H), and ^2J(Pt−H) coupling constant values of 55, 6.5, 33, 6.5, and 78 Hz, respectively. Once again, these are all reasonable for platinum(II) compounds. The monometalated species have similar spectra to one another, as do the bismetalated species when compared to each other. The monometalated species **16Mono** and **18Mono** were slightly contaminated with small amounts of the corresponding bismetalated species, which forms to a small extent. It proved difficult to separate the small amount of bis-species from the monoplatinum compounds with our attempts often leading to decomposition of the compounds.

PHOTOPHYSICAL MEASUREMENTS AND COMPUTATIONAL RESULTS

Time-Dependent Density Functional Theory and Density Functional Theory Calculations. The solid-state structure of **18Bis** (Figure 2) has a distorted square planar platinum(II) metal center with two C^N chelate ligands. There are two inequivalent molecules in the asymmetric unit; Figure 2 shows one of these. The dihedral angles between the planes defined by the Pt atom and the carbon and nitrogen atoms of each ligand in a molecule are 10.2 and 13.1° for the two molecules. The XRD data was used as input for our DFT study (see below), and the results have good agreement giving a dihedral angle of 11.2° (Figure S1). The platinum-carbon and platinum−nitrogen bond lengths are typical for platinum(II) species.[36,37]

The photophysical properties of the compound were examined and are summarized in Table 1. The absorbance spectra (Figure 3) showed the lowest energy peak for the compounds to be between 390 and 560 nm. These peaks have extinction coefficients of around 10^3 to 10^4; thus, they were tentatively assigned as metal to ligand charge transfer (MLCT) peaks.[7] The bathochromic shift of 170−190 nm for the corresponding emission spectra support the assignment. The emission spectra have their maximum peaks between 600 and 700 nm. Shoulders are observed at higher energy and lower energy depending on the compound with no definitive pattern for mono versus bis species. For example, the **16** and **18** mono/bis species pairs had similar emission maxima, while the **15** pair had the bis species emitting at a longer wavelength. Interestingly, the **14Mono** had an additional emission peak at higher energy around 455 nm. This has been tentatively

Table 1. Photophysical Data for Platinum Compounds

complex	absorption λ_{max}/nm (ε/M^{-1} cm^{-1}) × 10^3	emission λ_{max}/nm	lifetime ns (χ^2)
14Mono	435 (2.4), 382 (5.6)	642, 598, 455	165 (1.03)[c]
15Mono	464 (4.6)	652, 551	158 (1.01)[b]
16Mono	431 (3.7), 413 (3.9)	676, 606	203 (1.19)[a]
18Mono	435 (3.4), 416 (3.8), 380 (5.3)	668, 596	234 (1.13)[b]
14Bis	515 (7.9), 431 (6.5), 413 (6.6)	750, 680	281 (0.942)[a]
15Bis	560 (3.1), 454 (5.5), 415 (8.5)	748, 731, 636	207 (1.04)[b]
16Bis	511 (9.7), 434 (8.0), 413 (8.3)	752, 679	261 (1.02)[b]
18Bis	517 (1.2), 434 (8.7), 415 (9.4)	734, 671	458 (1.02)[b]

[a] $\lambda_{excitation}$ = 405 nm. [b] $\lambda_{excitation}$ = 450 nm. [c] $\lambda_{excitation}$ = 365 nm.

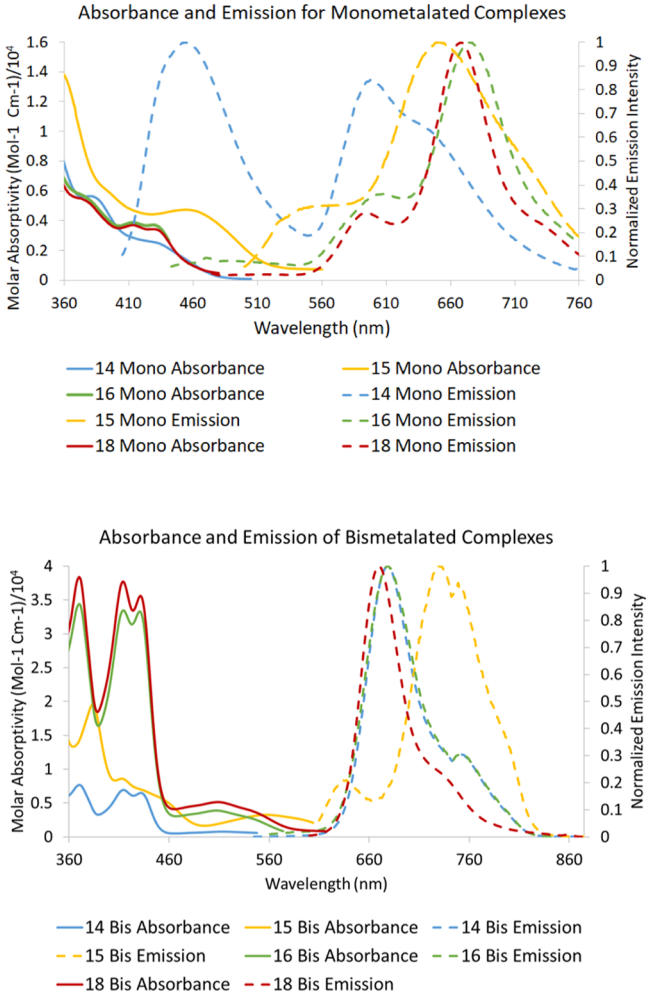

Figure 3. Absorption and emission spectra. Absorbance and normalized emission spectra for monometalated (top) and bismetalated compounds (bottom). [Samples] = 0.1 mM.

assigned to a fluorescence peak as it was determined to have an excited-state lifetime of 2.8 ns (χ^2 0.94).[7,38,39] Computational results (vide infra) corroborate a possible emission from S_1 to S_0 at approximately that energy. **15Mono** had a much smaller, similar emission band at around 400 nm. The other compounds did not have emission peaks with discernible features at higher energy. Generally, the bis species absorbed at a lower energy than the corresponding mono species, making the bathochromic shift slightly greater for the monospecies. **15Bis** has its spectrum red-shifted somewhat more compared

https://dx.doi.org/10.1021/acsomega.0c03993
ACS Omega 2020, 5, 26855−26863

to the others. Perhaps this can be attributed to its structural features in that it does not have a "spacer" between the naphthyl ring and the nitrogen. The lifetime measurements of the emission peaks listed in Table 1 yielded values of 150−450 ns, which are on the low end for phosphorescence,[40,41] which is expected for such compounds with MLCT bands; thus, our assignment is not unreasonable, given the data and the preponderance for such behavior for platinum(II) species, given their large spin−orbit coupling.[8,39] In order to help consolidate these tentative MLCT and phosphorescence assignments, a detailed time-dependent DFT (TD/DFT) study was undertaken for **18Bis**, the species for which an XRD structure determination has been obtained (vide supra).

DFT and TD-DFT were run on the **18Bis** compound as the results of the calculation could be directly compared to our crystallographic data. The structure of bismetalated **18Bis** was optimized and confirmed to represent an energetic minimum by harmonic frequency analysis. The agreement of the diffraction data bond lengths in the Pt(II) coordination sphere to theory was analyzed for a few different types of calculations (gas phase and solution phase, Table 2). The different

Table 2. Comparison of Solid-State SCXRD Pt Coordination Sphere Bond Lengths and DFT Gas-Phase and Solution-Phase Minimum Energy Geometries for 18Bis

bond	SCXRD (Å)	gas phase (Å)	DCM solution (Å)
Pt−C_1	1.9720	1.9901	1.9979
Pt−C_2	1.9528	1.9912	1.9974
Pt−N_1	2.1619	2.2406	2.2503
Pt−N_2	2.1387	2.2337	2.2467

calculation methodologies had very little impact on the optimized coordination environment for a single molecule, and the bond lengths appear to be systematically slightly longer in solution than those observed in the solid state. The calculation does reproduce the longer Pt−N versus Pt−C bond length, which is observed experimentally (Table 2).

In addition to analyzing the observed cis isomer (Figure 4) of **18Bis**, the structure and thermodynamics of the trans isomer were examined (Tables S1 and S2, Figure S2). Using the X-ray crystallographic structure as a rough starting point for representative bond distances, molecular mechanics were then used to generate reasonable input geometries for the trans isomer. Attempts were made to optimize the structure with

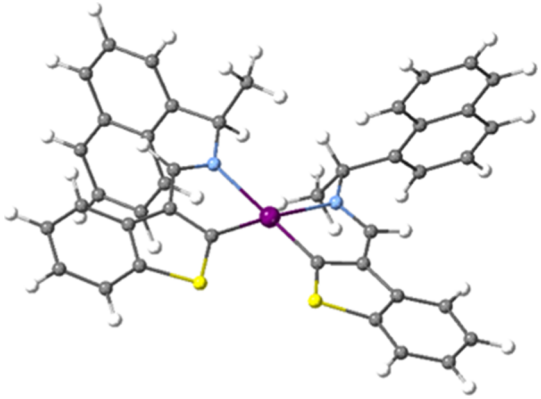

Figure 4. Gas-phase geometry-optimized structure of **18Bis** calculated at LACVP**/B3LYP DFT level of theory.

either trans or cis orientations of the *N*-α-methyls relative to the plane defined by the Pt(II) coordination sphere. The only structure which converged to a local minimum with no negative frequencies featured the former trans isomer, with the two different *N*-α-methyls pointed above or below the plane defined by the Pt(II) coordination sphere as is also seen experimentally in the observed cis isomer of **18Bis**. The data in solution indicate a greater thermodynamic stability for the cis isomer. Interestingly, the only structure which would converge if the *N*-α-methyls were both pointed in the same direction was a transition state featuring a single negative frequency which consisted of a rocking motion of one of the naphthalene ring which appeared to be a bond rotation away from the trans orientation of the two *N*-α-methyls. As expected, the stronger trans influence of the C donor ligand leads to a significantly increased C−Pt bond length in the hypothetical trans isomer and also a shorter N−Pt bond length.

TD-DFT and DFT calculations were run on **18Bis** to interrogate the nature of the observed electronic transitions in the UV−vis. DFT calculations on the frontier orbital manifold (HOMO − 5/LUMO + 5) show electron density concentrated largely on the platinum $5d_{xz}/d_{yz}$ orbitals in addition to the ligand π system in the HOMO manifold, while the LUMO manifold is of a more pronounced ligand π* character. Transitions between these orbitals which make up the observed visible absorption spectrum are generally of a mixed MLCT/ILCT character with electron density moving between the low-lying metal d orbitals and different parts of the ligand π* system (Figure S3, Chart S1, and Table S3). TD-DFT calculations simulate the major experimentally observed absorbance features (Figure 5).The large oscillator strength

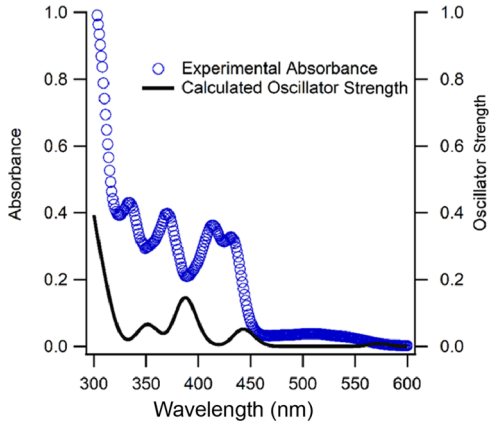

Figure 5. Observed UV−vis absorbance spectrum and simulated UV−vis spectrum from TD-DFT calculations for **18Bis**. The vertical excitations are broadened with a Gaussian function for visualization as described in experiment.

transitions, which make up the observed absorbance features, are principally described by a single major orbital transition (Figure S4). The (hole/particle) natural transition orbitals (NTOs) of these transitions are shown below which are well described by the principal contributing orbital transitions from comparison to DFT (Figure 6, Figure S5, and Table 3).[42]

CONCLUDING REMARKS

The reactions of $[Pt_2Me_4(\mu\text{-}SMe_2)_2]$ with a variety of benzothiophene-derived iminic ligands were conducted and sets of monometalated and bismetalated species were

https://dx.doi.org/10.1021/acsomega.0c03993
ACS Omega 2020, 5, 26855−26863

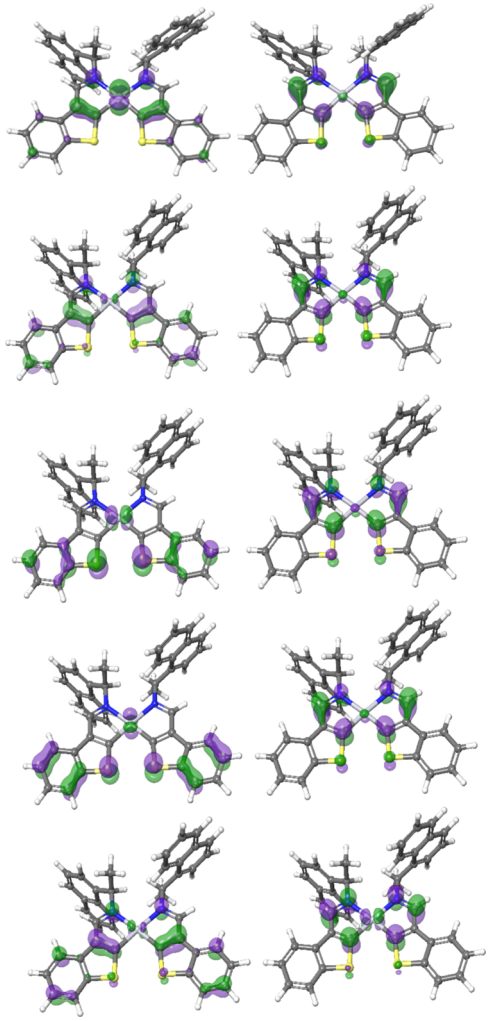

Figure 6. Hole (left) and particle (right) NTOs for S_1, S_2, S_5, S_8, and S_{14} transitions described in Table 3.

Table 3. TD-DFT-Calculated Vertical Excitations of High Oscillator Strength Transitions and Coefficients of Principle Contributing Orbital Transition

S_n	excitation energy (nm)	oscillator strength	principal contributing transitions	coefficient of principal contributing transition
S_1	572	0.008	HOMO to LUMO	0.93
S_2	443	0.052	HOMO − 1 to LUMO	0.99
S_5	388	0.136	HOMO − 4 to LUMO	0.98
S_8	351	0.060	HOMO − 5 to LUMO	0.97
S_{14}	306	0.164	HOMO − 1 to LUMO + 3	0.94

synthesized. The photophysical properties of the resulting compounds were recorded and analyzed. Tentative assignments due to intermediate values of the excited-state lifetime of the MLCT bands were reinforced with TD/DFT calculations. The TD/DFT calculations were invaluable in corroborating the tentative assignment.

EXPERIMENTAL SECTION

General. The solvents and reagents were purchased from Sigma-Aldrich unless otherwise noted. K_2PtCl_4 was purchased from the Pressure Chemical Company. NMR spectra were recorded at Bard College using Varian MR-400 MHz spectrometer (^{1}H, 400 MHz; ^{13}C, 100.6 MHz) and referenced to $SiMe_4$ (^{1}H, ^{13}C). Shifts are given in ppm and coupling constant J values in Hz. Abbreviations used: s = singlet; d = doublet; t = triplet; m = multiplet. Electrospray mass spectra were performed at Vassar College using an LC/MSD-TOF spectrometer. Elemental analyses have been included. Although several of these results are outside the range viewed as establishing analytical purity, they are provided to illustrate the best values obtained to date. A conscientious effort has been made to obtain pure compounds, where the values for the combustion analysis would fall within a range close to the theoretical values; however, the carbon values were at times high due to the presence of grease or solvents that could not be removed successfully from these organometallic compounds.

Computational Details. Calculations were carried out using TD-DFT and DFT implemented in the Jaguar 9.1 suite of ab initio quantum chemistry programs.[43] Geometry optimizations were performed with the B3LYP functional using a mixed basis set consisting of LANL2DZ with an effective core potential for the Pt atom and the 6-31-G** for all other atoms. X-ray crystallographic data was used as a starting point for geometries, which were confirmed to be energetic minima by vibrational analysis. In the case of the TD-DFT calculations, the UV−vis absorbance spectrum was simulated by optimization of the first 30 excited states and the use of a Poisson−Boltzmann implicit solvation model of dichloromethane to improve energetic agreement to the experimental UV−vis spectra. The resulting vertical excitation energies are convoluted with a Gaussian function of 20 nm half width for the purposes of visualization. Initial geometry guess was generated for the trans isomer using crystallographic data and molecular mechanics as implemented in Avogadro version 1.2.0 using the UFF force field. Figures of molecular structure output from calculations were generated using CrystalMaker software.[44] Initial geometry guess was generated using either crystallographic data molecular mechanics as implemented in Avogadro[45] version 1.2.0 using the UFF force field.

Photophysical Measurements. Steady-state emission spectra were recorded using a PTI QM-40 instrument with a PMT detector, which is sensitive up to 850 nm. In these experiments, the concentration of the platinum complexes ranged from 2×10^{-8} to 1×10^{-6} M. The luminescence lifetimes of the complexes were measured by time-correlated single-photon counting following excitation with a 365, 405, or 450 nm LED in methylene chloride. Samples were de-gassed for 5 min.

X-ray Diffraction. **18Bis** was crystallized by slow diffusion of pentane into an acetone solution. XRD data were collected on a Bruker APEX 2 CCD platform diffractometer [Mo Kα (l = 0.71073 Å)] at 125 K with crystals mounted on a nylon loop with Paratone-N cryo-protectant oil. After scaling with SADABS with Friedel opposites not treated as equivalent for scaling purposes, the structure of **18Bis** was solved using direct methods (SHELXS-97) and standard difference map techniques and was refined by full-matrix least-squares procedures on F2 with SHELXL-97.[46] All non-hydrogen atoms were refined anisotropically.

https://dx.doi.org/10.1021/acsomega.0c03993
ACS Omega 2020, 5, 26855−26863

Preparation of Compounds. Platinum dimer, *cis*-$[Pt_2Me_4(\mu\text{-}SMe_2)_2]$, **PtA**, was prepared as reported elsewhere.[47] Please see the Supporting Information section for additional experimental details, including NMR spectra, UV−vis spectra, and emission spectra.

Ligand 14 *[$(C_8H_5S)CH{=}NCH_2(C_{10}H_7)$]*. Benzothiophene-3-carboxaldehyde (0.3246 g, 0.0017 mol) and 1-naphthyl methylamine (0.3175 g, 0.002 mol) were dissolved in 30 mL of ethanol. The resulting solution was heated under reflux for 4 h. The solvent was removed with a rotary evaporator, and the resulting tan solid was washed with pentane and dried under vacuum. The product was characterized by ^{1}H NMR and ^{13}C NMR spectroscopy. Yield: 91% (0.46 g, 0.0015 mol). ^{1}H NMR (400 MHz, $CDCl_3$): δ 5.31 (s, 2H, CH_2), {7.24−8.83, aromatics}, and 8.68 (s, 1H, CH=N). ^{13}C NMR ($CDCl_3$): δ 62.8, 122.3, 123.9, 125.0, 125.2, 125.2, 125.5, 125.6, 125.6, 126.0, 127.7, 128.6, 132.9, and 156.7.

Ligand 15 *[$(C_8H_5S)CH{=}NCH(C_{10}H_7)$]*. Benzothiophene-3-carboxaldehyde (0.3877 g, 0.002 mol) and 2-naphthylamine (0.3477 g, 0.002 mol) were dissolved in 20.0 mL of ethanol. The resulting solution was heated under reflux for 4 h and then allowed to spin overnight at room temperature. A tan powder precipitate occurred, was washed with pentane, and dried under vacuum. The product was characterized by ^{1}H NMR and ^{13}C NMR spectroscopy. Yield: 90% (0.51 g, 0.0017 mol). ^{1}H NMR (400 MHz, $CDCl_3$): δ 8.84 (s, 1H, CH=N), {6.91−9.02 aromatics}. ^{13}C NMR ($CDCl_3$): δ 117.5, 121.2, 122.4, 125.2, 125.3, 125.5, 126.3, 127.7, 127.8, 128.9, 131.9, 134.1, 134.2, 134.9, 136.4, 140.8, 150.0, and 154.8.

Ligand 16 *[(S)-$(C_8H_5S)CH{=}NCHCH_3(C_{10}H_7)$]*. Benzothiophene-3-carboxaldehyde (0.2168 g, 0.0001000 mol) and (*S*)-1-(2-naphthyl)-ethylamine (0.228 g, 0.00100 mol) were dissolved in 30 mL of ethanol. The solution was heated and refluxed for 1.5 h and allowed to cool to room temperature. The solution was stirred overnight at room temperature under argon atmosphere. The solvent was removed with a rotary evaporator. The resulting orange powder was washed with pentane and dried under vacuum. The product was characterized by ^{1}H NMR and ^{13}C NMR spectroscopy. Yield: 83% (0.26 g, 8.3 × 10^{-4} mol). ^{1}H NMR (400 MHz, $CDCl_3$): δ 1.69 (d, J(H−H) = 6.7 Hz, 3H, CH_3), 4.64 (q, J(H−H) = 6.7 Hz, 1H, CH), {7.23−8.94 aromatics}, and 8.68 (s, 1H, CH=N). ^{13}C NMR ($CDCl_3$): δ 25.3, 70.6, 122.3, 124.8, 125.0, 125.2, 125.3, 125.4, 125.5, 125.9, 127.6, 127.8, 128.1, 132.6, 142.9, and 154.2.

Ligand 18 *[(R)-$(C_8H_5S)CH{=}NCHCH_3(C_{10}H_7)$]*. Benzothiophene-3-carboxaldehyde (0.3093 g, 0.0019 mol) and *R*-(+)-1-(1-naphthyl) ethylamine (0.3264 g, 0.0019 mol) were dissolved in 30 mL of ethanol. The solution was heated and refluxed for 4.0 h and allowed to cool to room temperature. The solution was stirred overnight at room temperature under argon atmosphere. The solvent was removed with a rotary evaporator. The resulting white powder was washed with pentane and dried under vacuum. The solid was characterized by ^{1}H NMR and ^{13}C NMR spectroscopy. Yield: 58% (0.347 g, 0.0011 mol). ^{1}H NMR (400 MHz, $CDCl_3$): δ 1.77 (d, J(H−H) = 6.8 Hz, 3H, CH_3), 5.32 (q, J(H−H) = 6.8 Hz, 1H, CH), {7.23−9.02 aromatics}, and 8.69 (s, 1H, CH=N). ^{13}C NMR ($CDCl_3$): δ 25.0, 66.8, 122.3, 123.6, 124.0, 125.0, 125.2, 125.3, 125.4, 125.7, 127.7,128.9, 130.6, 132.8, 134.0, 134.1, 136.7, 140.8, 141.4, and 154.4.

14Mono *[$PtCH_3S(CH_3)_2${$(C_8H_5S)CH{=}NCH_2(C_{10}H_7)$}]*. **PtA**, $[Pt_2(CH_3)_4(\mu\text{-}S(CH_3)_2)_2]$ (0.0455 g, 7.93 × 10^{-5}) and **Ligand 14** $[(C_8H_5S)CH{=}NCH_2(C_{10}H_7)]$ (0.0491, 1.63 × 10^{-4} mol) were dissolved in 30 mL of acetone. The resulting mixture was then allowed to stir at room temperature for 3.5 h. The solvent was removed by rotary evaporation. The resulting orange solid was characterized by ^{1}H NMR and ^{13}C NMR spectroscopy. Yield: 68% (0.30 g, 5.39 × 10^{-5} mol). ^{1}H NMR (400 MHz, $CDCl_3$): δ 1.24 (s, ^3J(Pt−H) = 78.4 Hz, 3H, Pt−CH_3), 2.02 (s, ^2J(Pt−H) = 31.6 Hz, 6H, SMe_2), 5.55 (s, ^3J(Pt−H) = 11.9 Hz, 2H, CH_2), {7.12−8.02 aromatics}, and 8.67 (s, ^3J(Pt−H) = 52.7 Hz, 1H, CH=N). ^{13}C NMR ($CDCl_3$): δ 20.0, 58.9, 118.7, 121.6, 122.6, 122.8, 124.4, 124.6, 125.0, 125.4, 125.9, 126.4, 127.9, 128.9, 130.6, 133.5, 133.9, 142.2, 166.6, and 174.5. (^{1}H−H)-2D-COSY-NMR-cross peaks: (5.54, 8.68)-(CH_2 to CH=N). (^{1}H−H)-2D-NOESY-NMR-cross peaks: (1.24, 2.01)-($PtCH_3$ to SMe_2), (8.67, 5.54)-(CH_2 to CH=N). Elemental analysis % calcd for $[C_{23}H_{23}NPtS_2]$: C, 48.23; H, 4.05; N, 2.45. Found: C, 50.96; H, 3.84; N, 2.56. ESI-HR-MS (m/z): found, 557.0733, calcd for $[C_{23}H_{23}NPtS_2{-}CH_3]^+$, 557.0685.

15Mono *[$PtCH_3S(CH_3)_2${$(C_8H_5S)CH{=}N(C_{10}H_7)$}]*. **PtA**, $[Pt_2(CH_3)_4(\mu\text{-}S(CH_3)_2)_2]$ (0.19 g, 5.6 × 10^{-5} mol) and **Ligand 15** $[(C_8H_5S)CH{=}NCH(C_{10}H_7)]$ (0.1951 g, 5.667 × 10^{-4} mol) were dissolved in 30 mL of acetone. The solution was heated under reflux for an hour and a half and then allowed to stir overnight under inert atmosphere. The solvent was removed with a rotary evaporator. The resulting solid was washed with pentane and dried under vacuum. The final product was characterized by ^{1}H NMR and ^{13}C NMR spectroscopy, yield: 43.8% (0.11 g, 3.83 × 10^{-3} mol). ^{1}H NMR (400 MHz, $CDCl_3$): δ 1.33 (s, ^2J(Pt−H) = 80.8 Hz, 3H, $PtCH_3$), 2.13 (s, ^3J(Pt−H) = 30.0 Hz, 6H, SMe_2), {7.13−8.03 aromatics}, and 8.75 (s, ^3J(Pt−H) = 49.5 Hz, 1H, CH=N). ^{13}C NMR ($CDCl_3$): δ −19.5, 20.4, 118.7, 119.5, 122.0, 122.5, 122.8, 124.7, 125.8, 126.7, 127.7, 127.8, 128.9, 131.9, 133.7, 138.6, 142.0, 148.7, and 164.9. Elemental analysis % calcd for $C_{22}H_{21}NPtS_2$: C, 47.30; H, 3.79; N, 2.51. Found: C, 48.58; H, 3.51; N, 2.67. ESI-HR-MS (m/z): found, 543.0559; calcd for $[C_{22}H_{21}NPtS_2{-}CH_3]^+$, 543.0528.

16Mono *[$PtCH_3S(CH_3)_2${(S)-$(C_8H_5S)CH{=}NCHCH_3(C_{10}H_7)$}]*. **PtA**, $[Pt_2(CH_3)_4(\mu\text{-}S(CH_3)_2)_2]$ (0.0260 g, 4.50 × 10^{-5} mol) and **Ligand 16** $[(S)\text{-}(C_8H_5S)CH{=}NCHCH_3(C_{10}H_7)]$ (0.0311 g, 9.06 × 10^{-5} mol) were dissolved in 10 mL of acetone. The solution was placed in a CEM microwave for 10 min at 80 °C. The solvent was removed with a rotary evaporator. The resulting orange solid was washed with pentane and dried under vacuum. The final product was characterized by ^{1}H NMR and ^{13}C NMR spectroscopy. Yield: 75% (0.010 g, 3.3 × 10^{-5} mol) ^{1}H NMR (400 MHz, $CDCl_3$): δ 1.16 (s, ^2J(Pt−H) = 78.8 Hz, 3H, $PtCH_3$, 3H, α-CH_3), 1.86 (s, ^3J(Pt−H) = 31.8 Hz, 6H, SMe_2), 1.87 (d, J(H−H) = 6.9 Hz), 5.51 (q, J(H−H) = 6.9 Hz, 1H, CH), {7.17−7.89 aromatics}, and 8.84 (s, ^3J(Pt−H) = 54.2 Hz, 1H, CH=N). ^{13}C NMR ($CDCl_3$): δ −19.7, 19.6, 21.6, 64.8, 110.6, 118.7, 121.7, 122.8, 124.3, 125.5, 125.6, 125.9, 126.2, 126.4, 126.5, 127.5, 128.0, 128.1, 133.2, 139.5, and 162.34. (^{1}H−H)-2D-NOESY-NMR-cross peaks: (5.51, 1.87)-(CH to α-CH_3), (5.51−8.84)-(CH to CH=N). (^{1}H−H)-2D-COSY-NMR-cross peaks: (5.51−1.87)-(CH to α-CH_3), (5.51, 1.85)-(SMe_2 to CH). ESI-HR-MS (m/z): found, 571.0874, calcd for $[C_{24}H_{25}NPtS_2{-}CH_3]^+$, 571.0841.

18Mono *[$PtCH_3S(CH_3)_2${(R)-$(C_8H_5S)CH{=}NCHCH_3(C_{10}H_7)$}]*. **PtA**, $[Pt_2(CH_3)_4(\mu\text{-}S(CH_3)_2)_2]$ (0.0235 g, 4.0 × 10^{-5}) and **Ligand 18** $[(R)\text{-}(C_8H_5S)CH{=}NCHCH_3(C_{10}H_7)]$ (0.0261 g,

https://dx.doi.org/10.1021/acsomega.0c03993
ACS Omega 2020, 5, 26855−26863

8.2×10^{-5}) were dissolved in 20 mL of acetone. The resulting solution was heated under reflux for 1 h, cooled to room temperature, and then was allowed to stir overnight. The solvent was removed with a rotary evaporator, and the resulting orange solid was washed with pentane and dried under vacuum. The final product was characterized by ^{1}H NMR and ^{13}C NMR spectroscopy. Yield: 95% (0.020 g, 3.75×10^{-5} mol). ^{1}H NMR (400 MHz, $CDCl_3$): δ 1.19 (s, ^3J(Pt−H) = 78.3 Hz, 3H, $PtCH_3$), 1.86 (d, J(H−H) = 6.6 Hz 3H, α-CH_3), 1.91 (m, ^3J(Pt−H) = 33.2, 3H SMe_2), 6.10 (q, ^3J(H−H) = 6.6 Hz, 1H, CH), {7.1−8.13 aromatics}, and 8.74 (s, ^3J(Pt−H) = 54.7 Hz, 1H, CH═N). ^{13}C NMR ($CDCl_3$): δ 19.7, 20.9, 59.3, 118.7, 121.5, 122.8, 123.5, 124.0, 124.2, 125.4, 125.6, 126.5, 128.1, 128.8, 130.7, 133.8, 138.2, 138.3, and 161.3. (^{1}H−H)-2D-COSY-NMR-cross peaks: (6.10, 1.85)-(CH to α-CH_3). (^{1}H−H)-2D-NOESY-NMR-cross peaks: (6.10, 1.85)-(CH to α CH_3). ESI-HR-MS (m/z): found, 571.0889, calcd for $[C_{24}H_{25}NPtS_2-CH_3]^+$, 571.0841. Elemental analysis % calcd for $[C_{24}H_{25}NPtS_2]$: C, 49.14; H, 4.30; N, 2.39. Found: C, 51.98; H, 4.05; N, 2.53.

14Bis *$[Pt\{(C_8H_5S)CH{=}NCHCH_3(C_{10}H_7)\}_2]$*. **PtA**, $[Pt_2(CH_3)_4(\mu\text{-}S(CH_3)_2)_2]$ (0.0263 g, 4.58×10^{-5} mol) and **Ligand 14** $[(C_8H_5S)CH{=}NCH2(C_{10}H_7)]$ (0.0555 g, 1.84×10^{-4} mol) were dissolved in toluene (12 mL). The resulting solution was heated under reflux for 4 h under inert conditions. The reaction mixture was cooled to room temperature and kept in the flask without stirring for 12 h. The resultant orange-red precipitate was separated by vacuum filtration and washed with 3 × 10 mL portions of diethyl ether. Yield: 98% (0.0365 g, 4.5×10^{-5} mol). ^{1}H NMR (400 MHz, $CDCl_3$): δ 5.04 (s, 2H, CH_2), {7.90−6.92, aromatics}and 8.22 (s, ^3J (Pt−H) = 70.4 Hz, 1H, CH═N). ^{13}C NMR ($CDCl_3$): δ 60.5, 110.6, 118.6, 122.1, 122.2, 122.5, 124.5, 124.9, 125.5, 125.9, 126.4, 128.0, 128.5, 130.0, 133.4, 133.8, and 169.4. (^{1}H−H)-2D-COSY-NMR-cross peaks: (5.04, 8.22)-(CH_2 to CH═N). (^{1}H−H)-2D-NOESY-NMR-cross peaks: (5.05, 8.22)-(CH_2 to CH═N). ESI-HR-MS (m/z): ound, 796.1475, calcd for $[C_{40}H_{28}N_2PtS_2+ H]^+$, 796.1421. Elemental analysis % calcd for $C_{40}H_{28}N_2PtS_2$: C, 60.37; H, 3.55; N, 3.52. Found: C, 59.54; H, 3.52; N, 3.57.

15Bis *$[Pt\{(C_8H_5S)CH{=}NCHCH_3(C_{10}H_7)\}_2]$*. **PtA**, $[Pt_2(CH_3)_4(\mu\text{-}S(CH_3)_2)_2]$ (0.023 g, 4.01×10^{-5} mol) and **Ligand 15** $[(C_8H_5S)CH{=}NCH_2(C_{10}H_7)]$ (0.0491 g, 1.71×10^{-4} mol) were dissolved in dry toluene (12 mL). The resulting mixture was heated to reflux for 4 h under argon. The reaction mixture was cooled to room temperature and kept in the flask without stirring for 12 h. Toluene was removed via rotary evaporation, and the product was triturated with diethyl ether and vacuum filtered. Yield: 85% (0.0255 g, 3.3×10^{-5}). ^{1}H NMR (400 MHz, $CDCl_3$): δ {6.79−7.94, aromatics} and 8.51 (s, ^3J(Pt−H) = 66.5 Hz, 1H, CH═N). ^{13}C NMR ($CDCl_3$): δ 110.3, 118.9, 119.2, 121.0, 122.5, 122.6, 125.2, 125.3, 126.0, 127.0, 127.2, 128.1, 129.0, 131.2, 133.0, 137.8 143.5, 147.4, and 168.2. ESI-HR-MS (m/z): found, 768.1148, calcd for $[C_{38}H_{24}N_2PtS_2+H]^+$, 768.1108.

16Bis *$[Pt\{(S)\text{-}(C_8H_5S)CH{=}NCHCH_3(C_{10}H_7)\}_2]$*. **PtA**, $[Pt_2(CH_3)_4(\mu\text{-}S(CH_3)_2)_2]$ (0.0244 g, 4.173×10^{-5} mol) and **Ligand 16** $[(S)\text{-}(C_8H_5S)CH{=}NCH_2(C_{10}H_7)]$ (0.0526 g, 1.67×10^{-4} mol) were dissolved in toluene (12 mL). The resulting solution was heated under reflux for 4 h under argon. The reaction mixture was cooled to room temperature and kept in the flask without stirring for 12 h. The reaction mixture was vacuum filtered to separate a very small amount of precipitate. The filtrate had its solvent removed via rotary evaporation, triturated with diethyl ether, and vacuum filtered. Yield: 65% (0.022 g, 2.7×10^{-5} mol) ^{1}H NMR (400 MHz, $CDCl_3$): δ 1.77 (d, J(H−H) = 6.7 Hz, 3H, CH_3), 5.47 (q, J(H−H) = 6.7 Hz, 1H, CH), {7.15−7.9 aromatics}, and 8.32 (s, ^3J(Pt−H) = 71.5 Hz, 1H CH═N). ^{13}C NMR ($CDCl_3$): δ 21.4, 63.1, 118.2, 122.1, 122.4, 124.7, 125.8, 125.9, 126.3, 126.5, 127.6, 128.2, 128.9, 132.8, 133.3, 137.2, 138.5, 141.9, 143.6, 164.2, and 166.2. (^{1}H−H)-2D-COSY-NMR-cross peaks, (5.49, 1.76)-(CH to α-CH_3). (^{1}H−H)-2D-NOESY-NMR-cross peaks, (5.46−1.75)-(CH to α CH_3). ESI-HR-MS (m/z): found, 823.1675, calcd for $C_{42}H_{32}N_2PtS_2$, 823.1655. Elemental analysis % calcd for $C_{42}H_{32}N_2PtS_2$: C, 61.23; H, 3.91; N, 3.40. Found: C, 60.58; H, 3.66; N, 3.34.

18Bis *$[Pt\{(R)\text{-}(C_8H_5S)CH{=}NCHCH_3(C_{10}H_7)\}_2]$*. **PtA**, $[Pt_2(CH_3)_4(\mu\text{-}S(CH_3)_2)_2]$, (0.0205 g, 3.56×10^{-5} mol) and **Ligand 18** $[(R)\text{-}(C_8H_5S)CH{=}NCHCH_3(C_{10}H_7)]$ (0.0421 g, 1.33×10^{-4}) were dissolved in 15 mL of toluene. The resulting solution was heated under reflux for 4 h under argon. The solution was allowed to stir at room temperature overnight. The resultant dark red precipitate was separated via vacuum filtration and washed with diethyl ether. Product was characterized by NMR spectroscopy. Yield: 72% (0.021 g, 2.54×10^{-5} mol). ^{1}H NMR (400 MHz, $CDCl_3$): δ 1.80 (d, ^3J(H−H) = 6.5 Hz, 3H, CH_3), 6.06 (q, J(H−H) = 6.5 Hz, 1H, CH), and {7.12−8.33 aromatics} 8.23 (s, ^3J(Pt−H) = 70.5 Hz, 1H, CH═N). ^{13}C NMR ($CDCl_3$): δ 21.5, 60.8, 118.8, 122.2, 122.5, 124.5, 124.8, 125.1, 125.3, 126.1, 127.2, 129.1, 129.3, 131.0, 134.5, 137.3, and 165.5. (^{1}H−H)-2D-COSY-NMR-cross peaks, (6.04, 1.80)-(CH to CH_3). (^{1}H−H)-2D-NOESY-NMR-cross peaks, (6.04, 8.26)-(CH to CH═N), (6.03, 1.80)-(CH to CH_3). ESI-HR-MS (m/z): found, 824.1793, calcd for $[C_{42}H_{32}N_2PtS_2+H]^+$, 824.1734. Elemental analysis % calcd for $C_{42}H_{32}N_2PtS_2$: C, 61.23; H, 3.91; N, 3.40. Found: C, 60.03; H, 3.70, N; 3.26.

■ ASSOCIATED CONTENT

Supporting Information

The Supporting Information is available free of charge at https://pubs.acs.org/doi/10.1021/acsomega.0c03993.

Molecular structures illustrating planes for both molecules in the asymmetric unit and planes in calculated structure; cis and trans isomer energy comparisons; gas-phase geometry-optimized structure of the trans isomer of 18Bis; coordination sphere bond lengths and DFT gas-phase and solution-phase minimum energy geometries for hypothetical trans isomer of **18Bis**; orbitals at and below HOMO and orbitals at and above LUMO; energy levels and energy values determined for frontier and near-frontier orbitals; observed theoretical spectrum arising from four high oscillator strength transitions; and natural transition orbitals for the high oscillator strength transitions; NMR spectra; Uv−vis spectra; Emission Spectra (PDF)

CCDC for compound **18Bis** (CIF)

■ AUTHOR INFORMATION

Corresponding Author

Craig M. Anderson − *Department of Chemistry, Bard College, Annandale-on-Hudson, New York 12504, United States;* orcid.org/0000-0001-5875-4380; Phone: 845-752-2356; Email: canderso@bard.edu; Fax: 845-752-2339

Authors

Belle Coffey − *Department of Chemistry, Bard College, Annandale-on-Hudson, New York 12504, United States*

Leslie Morales − *Department of Chemistry, Bard College, Annandale-on-Hudson, New York 12504, United States*

Matthew W. Greenberg − *Department of Chemistry, Bard College, Annandale-on-Hudson, New York 12504, United States*

Matthew Norman − *Department of Chemistry, Bard College, Annandale-on-Hudson, New York 12504, United States*

Michael Weinstein − *Department of Chemistry, Bard College, Annandale-on-Hudson, New York 12504, United States*

Garrett Brown − *Department of Chemistry, Bard College, Annandale-on-Hudson, New York 12504, United States*

Joseph M. Tanski − *Department of Chemistry, Vassar College, Poughkeepsie, New York 12604, United States*

Complete contact information is available at: https://pubs.acs.org/10.1021/acsomega.0c03993

Notes

The authors declare no competing financial interest.

■ ACKNOWLEDGMENTS

This material is based upon work supported by the US National Science Foundation under CHE-1665435 (C.M.A., P.I.). We also thank the Bard Summer Research Institute (BSRI) for support. Mass spectrometry was run at Vassar College with the help of Karen Wovkulich. We thank Prof. Christopher LaFratta of Bard College for help in obtaining photophysical data.

■ REFERENCES

(1) Lázaro, A.; Cunha, C.; Bosque, R.; Pina, J.; Ward, J. S.; Truong, K.-N.; Rissanen, K.; Lima, J. C.; Crespo, M.; Seixas de Melo, J. S.; Rodríguez, L. Room-Temperature Phosphorescence and Efficient Singlet Oxygen Production by Cyclometalated Pt(II) Complexes with Aromatic Alkynyl Ligands. *Inorg. Chem.* **2020**, *59*, 8220−8230.

(2) Wang, G.-W.; Wheatley, M.; Simonetti, M.; Cannas, D. M.; Larrosa, I. Cyclometalated Ruthenium Catalyst Enables Ortho-Selective C−H Alkylation with Secondary Alkyl Bromides. *Chem* **2020**, *6*, 1459−1468.

(3) Kim, M. S.; Yun, D.; Chae, J. B.; So, H.; Lee, H.; Kim, K.-T.; Kim, M.; Lim, M. H.; Kim, C. A Novel Thiophene-Based Fluorescent Chemosensor for the Detection of Zn2+ and CN−: Imaging Applications in Live Cells and Zebrafish. *Sensors* **2019**, *19*, 5458.

(4) Abbas, S.; Din, I. u. D.; Raheel, A.; Tameez ud Din, A. Cyclometalated Iridium (III) Complexes: Recent Advances in Phosphorescence Bioimaging and Sensing Applications. *Appl. Organomet. Chem.* **2020**, *34*, 1−16.

(5) Albrecht, M. Cyclometalation Using D-Block Transition Metals: Fundamental Aspects and Recent Trends. *Chem. Rev.* **2010**, *110*, 576−623.

(6) Zhang, X.; Hou, Y.; Xiao, X.; Chen, X.; Hu, M.; Geng, X.; Wang, Z.; Zhao, J. Recent Development of the Transition Metal Complexes Showing Strong Absorption of Visible Light and Long-Lived Triplet Excited State: From Molecular Structure Design to Photophysical Properties and Applications. *Coord. Chem. Rev.* **2020**, *417*, 213371.

(7) Kozhevnikov, V. N.; Durrant, M. C.; Williams, J. A. G. Highly Luminescent Mixed-Metal Pt(II)/Ir(III) Complexes: Bis-Cyclometalation of 4,6-Diphenylpyrimidine as a Versatile Route to Rigid Multimetallic Assemblies. *Inorg. Chem.* **2011**, *50*, 6304−6313.

(8) Medlycott, E. A.; Hanan, G. S.; Medlycott, E. A.; Hanan, G. S. Enhanced Room Temperature Luminescence Lifetimes. *Chem. Soc. Rev.* **2003**, *44*, 1−10.

(9) Gaspar, H.; Figueira, F.; Strutyński, K.; Melle-Franco, M.; Ivanou, D.; Tomé, J. P. C.; Pereira, C. M.; Pereira, L.; Mendes, A.; Viana, J. C.; Bernardo, G. Thiophene- and Carbazole-Substituted N-Methyl-Fulleropyrrolidine Acceptors in PffBT4T-2OD Based Solar Cells. *Materials* . **2020**, *13*. DOI: DOI: 10.3390/ma13061267.

(10) Tokárová, Z.; Maxianová, P.; Váry, T.; Nádaždy, V.; Végh, D.; Tokár, K. Thiophene-Centered Azomethines: Structure, Photophysical and Electronic Properties. *J. Mol. Struct.* **2020**, *1204*, 127492.

(11) Kolcu, F.; Erdener, D.; Kaya, İ. A Schiff Base Based on Triphenylamine and Thiophene Moieties as a Fluorescent Sensor for Cr (III) Ions: Synthesis, Characterization and Fluorescent Applications. *Inorg. Chim. Acta* **2020**, *509* (). DOI: DOI: 10.1016/j.ica.2020.119676.

(12) Yadav, S.; Dwivedi, V. K.; Gupta, S.; Surolia, A. Benzothiophenes as Potent Analgesics against Neuropathic Pain. *Adv. Exp. Med. Biol.* **2018**, *1112*, 245−254.

(13) Khalifa, M. E.; Almalki, A. S. A.; Merazga, A.; Mersal, G. A. M. Design, Molecular Modeling and Synthesis of Metal-Free Sensitizers of Thieno Pyridine Dyes as Light-Harvesting Materials with Efficiency Improvement Using Plasmonic Nanoparticles. *Molecules* . **2020**, *25*. DOI: DOI: 10.3390/molecules25081813.

(14) Sharmoukh, W.; Cong, J.; Ali, B. A.; Allam, N. K.; Kloo, L. Comparison between Benzothiadizole-Thiophene- And Benzothiadizole-Furan-Based D-A-π-A Dyes Applied in Dye-Sensitized Solar Cells: Experimental and Theoretical Insights. *ACS Omega* **2020**, *5*, 16856.

(15) Rao, G. H.; Pandey, M.; Narayanaswamy, K.; Srinivasa Rao, R.; Pandey, S. S.; Hayase, S.; Singh, S. P. Synthesis and Optoelectrical Characterization of Novel Squaraine Dyes Derived from Benzothiophene and Benzofuran. *ACS Omega* **2018**, *3*, 13919−13927.

(16) Walter, C.; Fallows, N.; Kesharwani, T. Copper-Catalyzed Electrophilic Chlorocyclization Reaction Using Sodium Chloride as the Source of Electrophilic Chlorine. *ACS Omega* **2019**, *4*, 6538−6545.

(17) Kim, S.; Dahal, N.; Kesharwani, T. Environmentally Benign Process for the Synthesis of 2,3-Disubstituted Benzo[b]Thiophenes Using Electrophilic Cyclization. *Tetrahedron Lett.* **2013**, *54*, 4373−4376.

(18) Kesharwani, T.; Giraudy, K. A.; Morgan, J. L.; Kornman, C.; Olaitan, A. D. Green Synthesis of Halogenated Thiophenes, Selenophenes and Benzo[b]Selenophenes Using Sodium Halides as a Source of Electrophilic Halogens. *Tetrahedron Lett.* **2017**, *58*, 638−641.

(19) Anderson, C. M.; Weinstein, M. A.; Morris, J.; Kfoury, N.; Duman, L.; Balema, T. A.; Kreider-Mueller, A.; Scheetz, P.; Ferrara, S.; Chierchia, M.; Tanski, J. M. Biscyclometalated Platinum Complexes with Thiophene Ligands. *J. Organomet. Chem.* **2013**, *723*, 188−197.

(20) Anderson, C. M.; Mastrocinque, C.; Greenberg, M. W.; McClellan, I. C.; Duman, L.; Oh, N.; Mastrocinque, F.; Pizzuto, M.; Tran, K.; Tanski, J. M. Synthesis, Characterization, and Photophysical Properties of Bismetalated Platinum Complexes with Benzothiophene Ligands. *J. Organomet. Chem.* **2019**, *882*, 10−17.

(21) Anderson, C. M.; Crespo, M.; Tanski, J. M. Synthesis and Reactivity of Coordination and Six-Membered, Cyclometalated Platinum Complexes Containing a Bulky Diimine Ligand. *Organometallics* **2010**, *29*, 2676−2684.

(22) Li, K.; Tong, G. S. M.; Yuan, J.; Ma, C.; Du, L.; Yang, C.; Kwok, W.-M.; Phillips, D. L.; Che, C.-M.; Che, C.-M. Excitation-Wavelength-Dependent and Auxiliary-Ligand-Tuned Intersystem-Crossing Efficiency in Cyclometalated Platinum(II) Complexes: Spectroscopic and Theoretical Studies. **2020**. DOI: DOI: 10.1021/acs.inorgchem.0c01192.

(23) Minenkov, Y.; Sharapa, D. I.; Cavallo, L. Application of Semiempirical Methods to Transition Metal Complexes: Fast Results but Hard-to-Predict Accuracy. *J. Chem. Theory Comput.* **2018**, *14*, 3428−3439.

(24) Niu, S.; Hall, M. B. Theoretical Studies on Reactions of Transition-Metal Complexes. *Chem. Rev.* **2000**, *100*, 353−406.

(25) Balcells, D.; Clot, E.; Eisenstein, O. C—H Bond Activation in Transition Metal Species from a Computational Perspective. *Chem. Rev.* **2010**, *110*, 749−823.
(26) Vogiatzis, K. D.; Polynski, M. V.; Kirkland, J. K.; Townsend, J.; Hashemi, A.; Liu, C.; Pidko, E. A. Computational Approach to Molecular Catalysis by 3d Transition Metals: Challenges and Opportunities. *Chem. Rev.* **2019**, *119*, 2453−2523.
(27) Gauthier, S.; Caro, B.; Robin-Le Guen, F.; Bhuvanesh, N.; Gladysz, J. A.; Wojcik, L.; Le Poul, N.; Planchat, A.; Pellegrin, Y.; Blart, E.; Jacquemin, D.; Odobel, F. Synthesis, Photovoltaic Performances and TD-DFT Modeling of Push-Pull Diacetylide Platinum Complexes in TiO_2 Based Dye-Sensitized Solar Cells. *Dalton Trans.* **2014**, *43*, 11233−11242.
(28) Han, D.; Wu, Y.; Cai, H.; Pang, C.; Zhao, L. DFT/TDDFT Investigation on the Electronic Structures and Photophysical Properties of a Series of Substituted N-Heterocyclic Carbene (NHC) Platinum(II) Complexes. *Synth. Met.* **2015**, *209*, 455−460.
(29) Liu, R.; Azenkeng, A.; Li, Y.; Sun, W. Long-Lived Platinum(Ii) Diimine Complexes with Broadband Excited-State Absorption: Efficient Nonlinear Absorbing Materials. *Dalton Trans.* **2012**, *41*, 12353−12357.
(30) Wu, W.; Wu, W.; Ji, S.; Guo, H.; Zhao, J. Accessing the Long-Lived Emissive ^{3}IL Triplet Excited States of Coumarin Fluorophores by Direct Cyclometallation and Its Application for Oxygen Sensing and Upconversion. *Dalton Trans.* **2011**, *40*, 5953−5963.
(31) Rendina, L. M.; Puddephatt, R. J. Oxidative Addition Reactions of Organoplatinum(II) Complexes with Nitrogen-Donor Ligands. *Chem. Rev.* **1997**, *97*, 1735−1754.
(32) Crespo, M. Fluorine in Cyclometalated Platinum Compounds. *Organometallics* **2012**, *31*, 1216−1234.
(33) Behnia, A.; Fard, M. A.; Puddephatt, R. J. Stereochemistry of Oxidative Addition of Methyl Iodide and Hydrogen Peroxide to Organoplatinum(II) Complexes Having an Appended Phenol Group and the Supramolecular Chemistry of the Platinum(IV) Products. *J. Organomet. Chem.* **2019**, *902*, 120962.
(34) Gandioso, A.; Valle-Sistac, J.; Rodríguez, L.; Crespo, M.; Font-Bardía, M. Platinum(II) Compounds Containing Cyclometalated Tridentate Ligands: Synthesis, Luminescence Studies, and a Selective Fluoro for Methoxy Substitution. *Organometallics* **2014**, *33*, 561−570.
(35) Crespo, M.; Font-Bardia, M.; Solans, X. Compound $[PtPh_2(SMe_2)_2]$ as a Versatile Metalating Agent in the Preparation of New Types of [C,N,N'] Cyclometalated Platinum Compounds. *Organometallics* **2004**, *23*, 1708−1713.
(36) Newkome, G. R.; Puckett, W. E.; Gupta, V. K.; Kiefer, G. E. Cyclometalation of the Platinum Metals with Nitrogen and Alkyl, Alkenyl, and Benzyl Carbon Donors. *Chem. Rev.* **1986**, *86*, 451−489.
(37) Melník, M.; Mikuš, P. Stereoisomers of Organoplatinum Complexes. *J. Organomet. Chem.* **2015**, *799−800*, 239−256.
(38) Rajendra Kumar, G.; Thilagar, P. Tuning the Phosphorescence and Solid State Luminescence of Triarylborane-Functionalized Acetylacetonato Platinum Complexes. *Inorg. Chem.* **2016**, *55*, 12220−12229.
(39) Kozhevnikov, D. N.; Kozhevnikov, V. N.; Shafikov, M. Z.; Prokhorov, A. M.; Bruce, D. W.; Gareth Williams, J. A. Phosphorescence vs Fluorescence in Cyclometalated Platinum(II) and Iridium(III) Complexes of (Oligo)Thienylpyridines. *Inorg. Chem.* **2011**, *50*, 3804−3815.
(40) Murphy, L. Luminescent Platinum Compounds: From Molecules to OLEDs. *Introduction to Thermoelectricity: Springer Series in Materials Science*; Bozec, H., Eds.; Topics in Organometallic Chemistry; Springer-Verlag, 2010; pp 75−111.
(41) Anderson, C.; Freedman, D. A.; Jennings, M.; Gray, B. Dimethylplatinum (II) Complexes with Isocyanocoumarin Ligands: The Crystal Structure of Cis-Dimethylbis-(7-Diethylamino-3-Isocyanocoumarin)Platinum(II). *J. Organomet. Chem.* **2005**, *690*, 168−176.
(42) Martin, R. L. Natural Transition Orbitals. *J. Chem. Phys.* **2003**, *118*, 4775−4777.
(43) Bochevarov, A. D.; Harder, E.; Hughes, T. F.; Greenwood, J. R.; Braden, D. A.; Philipp, D. M.; Rinaldo, D.; Halls, M. D.; Zhang, J.; Friesner, R. A. Jaguar: A High-Performance Quantum Chemistry Software Program with Strengths in Life and Materials Sciences. *Int. J. Quantum Chem.* **2013**, *113*, 2110−2142.
(44) MacRae, C. F.; Sovago, I.; Cottrell, S. J.; Galek, P. T. A.; McCabe, P.; Pidcock, E.; Platings, M.; Shields, G. P.; Stevens, J. S.; Towler, M.; Wood, P. A. Mercury 4.0: From Visualization to Analysis, Design and Prediction. *J. Appl. Crystallogr.* **2020**, *53*, 226−235.
(45) Hanwell, M. D.; Curtis, D. E.; Lonie, D. C.; Vandermeersch, T.; Zurek, E.; Hutchison, G. R. Avogadro: An Advanced Semantic Chemical Editor, Visualization, and Analysis Platform. *J. Cheminform.* **2012**, *4*, 1−17.
(46) Sheldrick, G. M. A Short History of SHELX. *Acta Crystallogr., Sect. A: Found. Crystallogr.* **2008**, *64*, 112−122.
(47) Scott, J. D.; Puddephatt, R. J. Ligand Dissociation as a Preliminary Step in Methyl for Halogen Exchange Reactions of Platinum(II) Complexes. *Organometallics* **1983**, *2*, 1643−1648.

https://dx.doi.org/10.1021/acsomega.0c03993
ACS Omega 2020, 5, 26855−26863